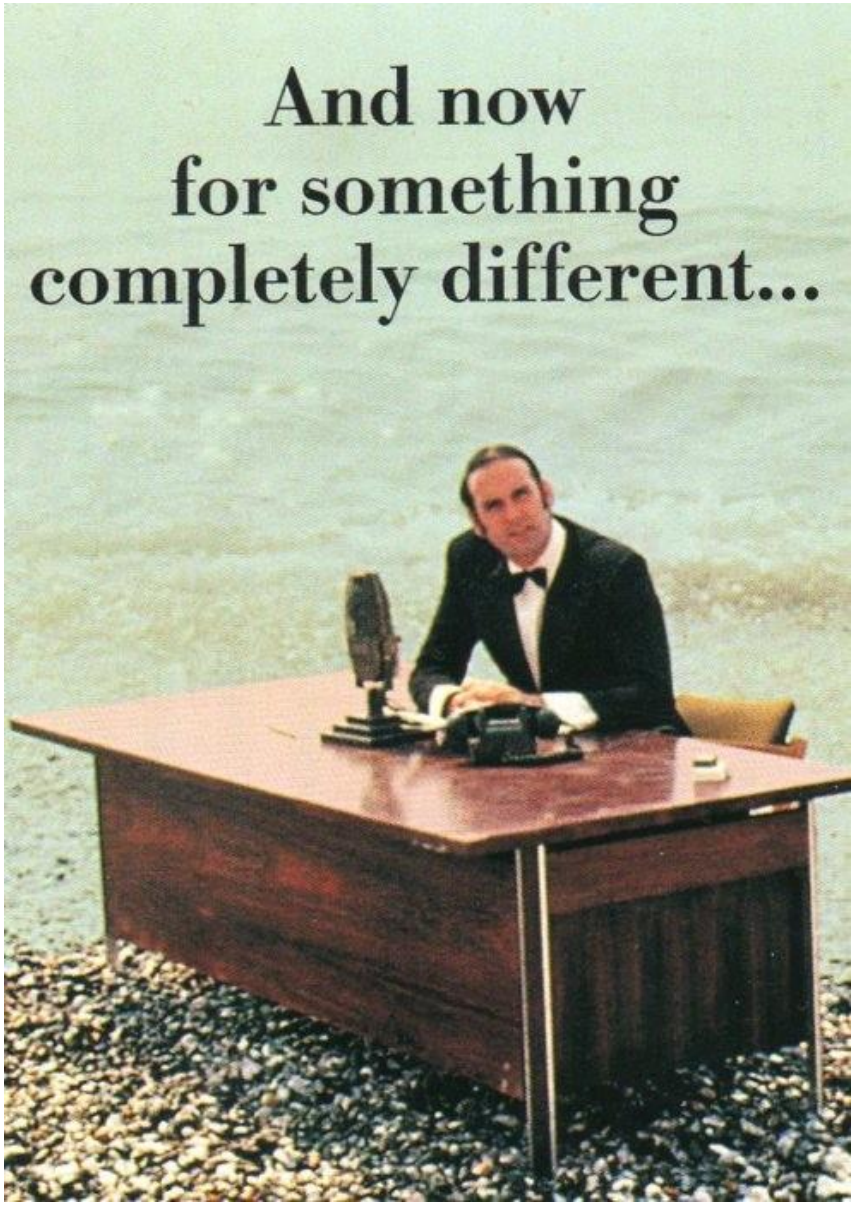

Hypermetallic molecules

(Picture courtesy of Python M)

An ab initio study of the alkaline earth oxides **BeOBe, MgOMg, CaOCa, SrOSr, BaOBa, and RaORa.**

Bojana Ostojić (Belgrade),
Per Jensen (Wuppertal),
Peter Schwerdtfeger (Massey University, New Zealand),
Phil Bunker (NRC, Ottawa).

"Hypermetallic" since they have one more metal atom than they should

PERIODIC TABLE OF ELEMENTS

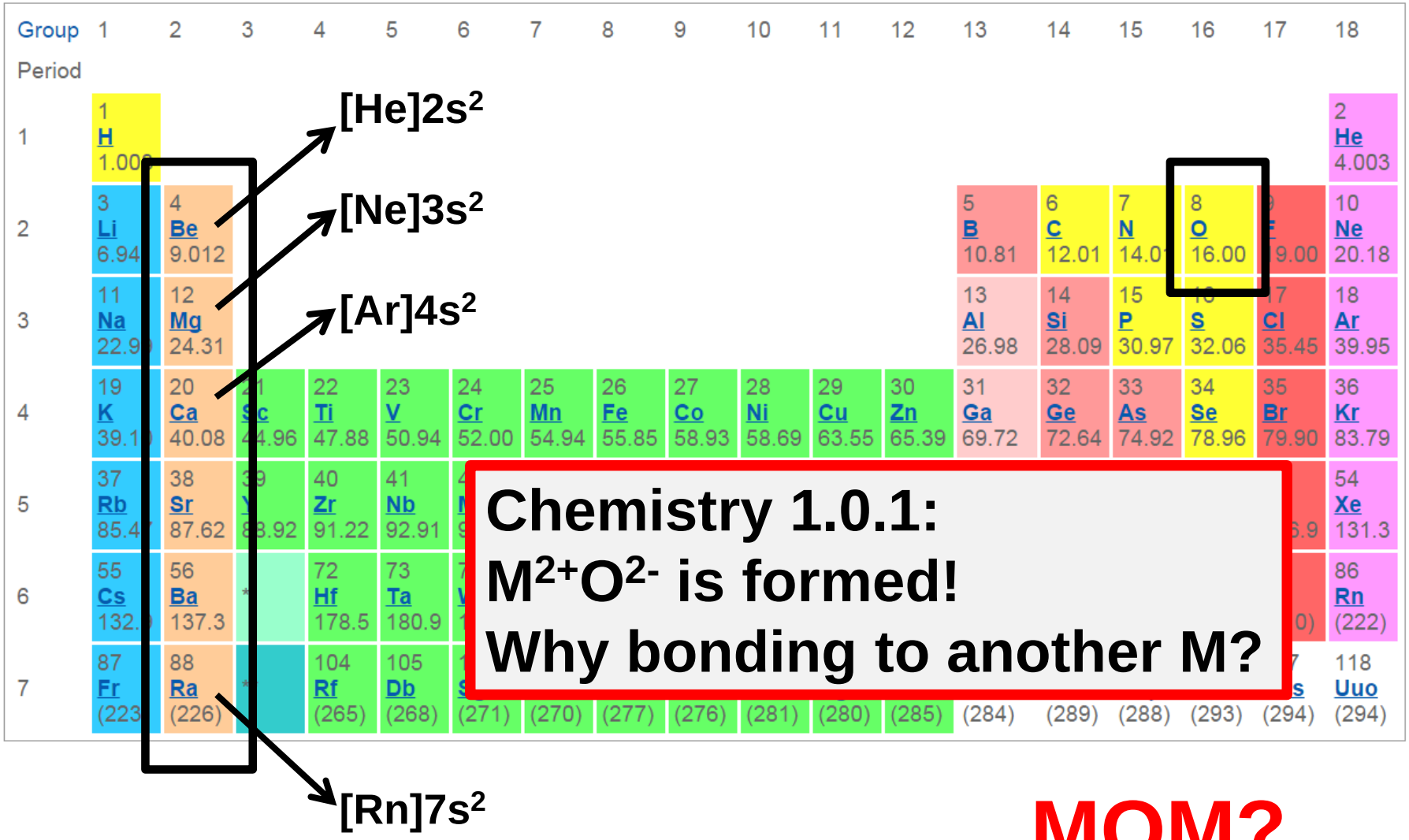

PERIODIC TABLE OF ELEMENTS

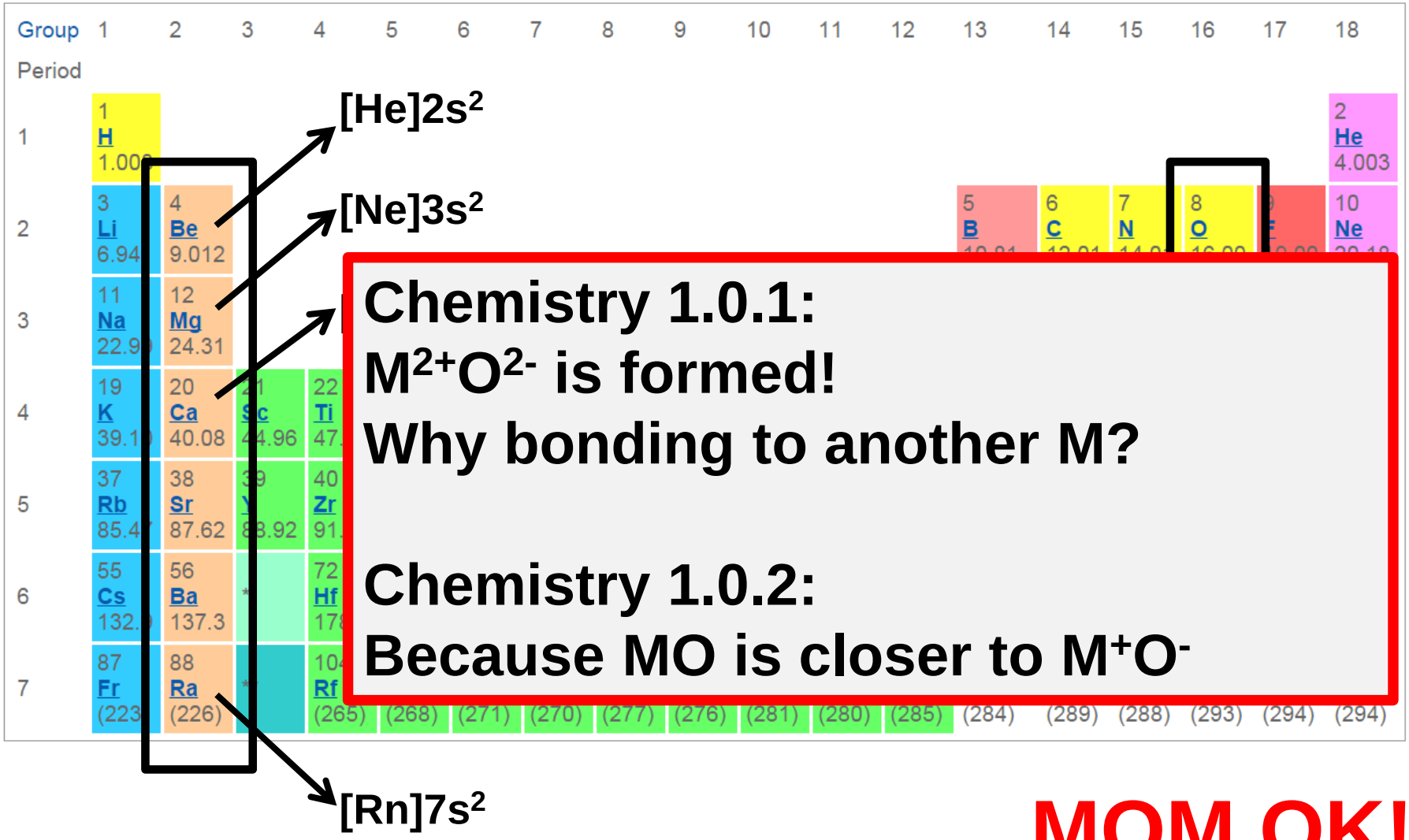

Chemistry 1.0.1:
$M^{2+}O^{2-}$ is formed!
Why bonding to another M?

Chemistry 1.0.2:
Because MO is closer to $M^{+}O^{-}$

MOM OK!

Apart from BeOBe, little known experimentally.

Our interest in these molecules is three-fold:

- To make precise ab initio calculations on them in order to understand the electronic structure,
- To predict the IR and electronic spectra and to compare with the experimental spectra,
- To calculate Singlet-Triplet splittings and S-T interaction strengths in order to test these molecules as candidates for high precision spectral measurements aimed at looking for a time-variation in M_p/m_e and fine structure constant α.

The *ab initio* slide

Please direct questions to
peter.schwerdtfeger@gmail.com

Molecule	Method	Basis set
BeOBe	CASSCF⇨MRCI	cc-pCVQZ
MgOMg	FV-CASSCF⇨MRCISD	cc-pCVQZ
CaOCa	FV-CASSCF⇨MRCISD+RS2C	cc-pwCVQZ-DK
SrOSr	CASSCF⇨MRCISD+RS2C	Sadlej pVTZ and Stuttgart relativistic small-core effective core potential for Sr
BaOBa and RaORa	CASSCF⇨MRCI	cc-pCVQZ and Stuttgart small-core relativistic effective core potential ECP46MDF and ECP78MDF for Ba and Ra

Nuclear-motion calculations and spectral simulations with MORBID

BeOBe, MgOMg, CaOCa, SrOSr, BaOBa, and RaORa.

We find that all these MOM molecules have

A linear $^{1}\Sigma_{g}^{+}$ ground electronic state and a fairly low lying linear $^{3}\Sigma_{u}^{+}$ first excited electronic state.

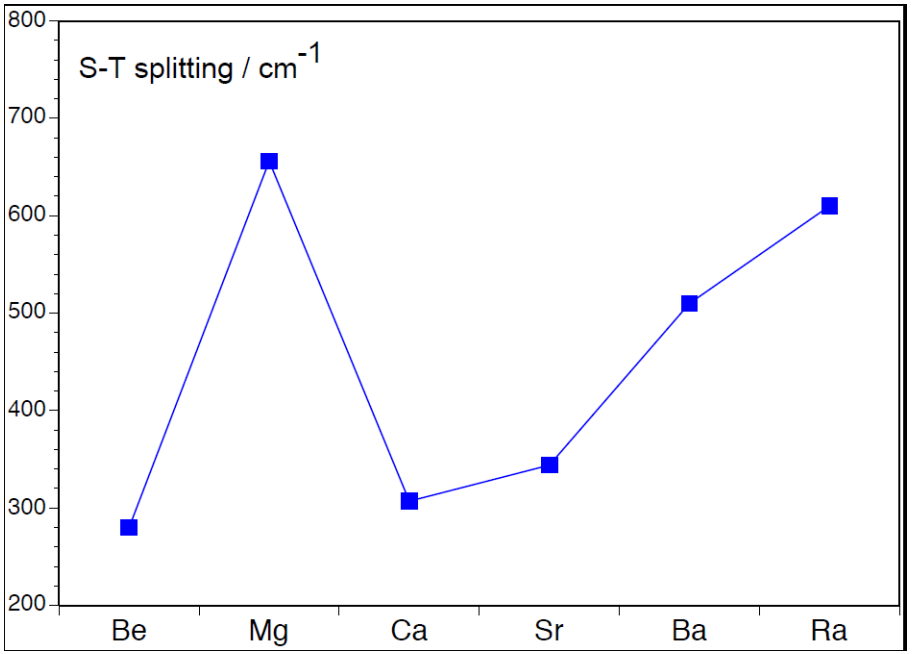

S-T spin-orbit coupling too small for them to be good candidates for use in measuring the time dependence of the fundamental parameters.

BeOBe bending potential curves

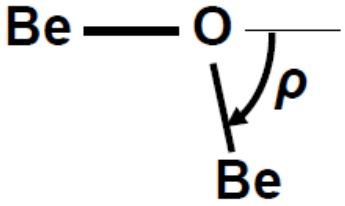

$T_e(\tilde{a}) = 293$ cm^{-1}

Singlet-triplet splitting

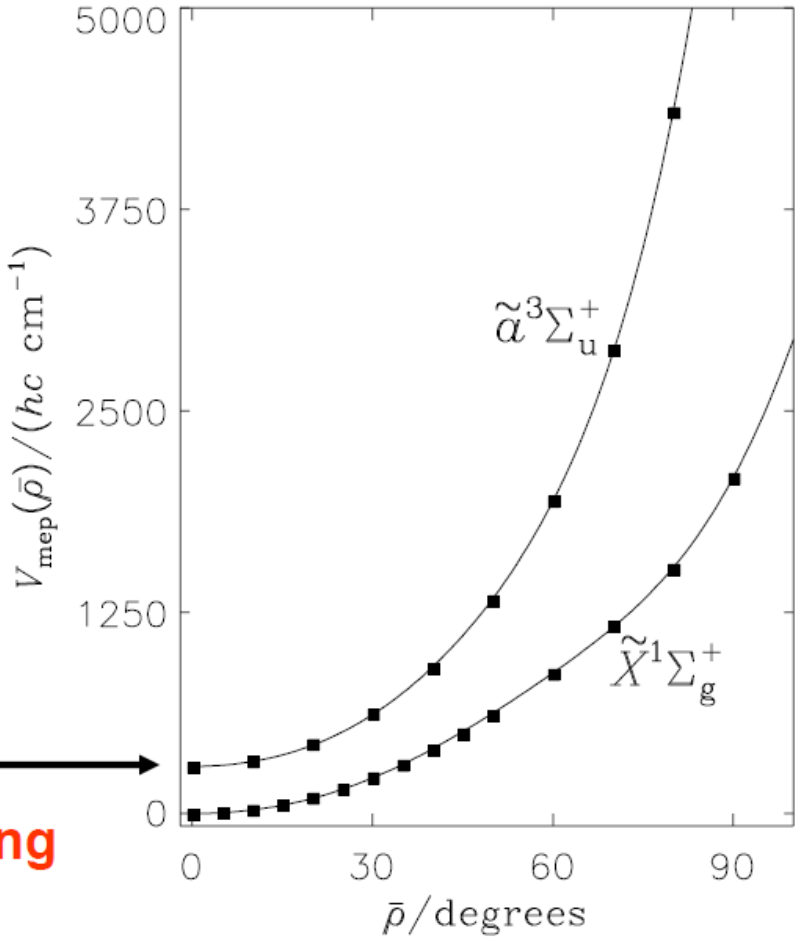

BeOBe

The calculated vibrational term values $G_{\rm vib} = E(v_1, v_2^{\ell_2}, v_3, N_{\rm min} = \ell_2) - E(0, 0^0, 0, 0)$ and effective rotational constants $B_{\rm eff}$ (in $\rm cm^{-1}$) for $\rm Be^{16}OBe$ in the electronic states $\tilde{X}\,^1\Sigma_g^+$ and $\tilde{a}\,^3\Sigma_u^+$.

exp

113

1039

1414

		$\tilde{X}\,^1\Sigma_g^+$		$\tilde{a}\,^3\Sigma_u^+$	
$(v_1, v_2^{\ell_2}, v_3)$	$N_{\rm min}$	$G_{\rm vib}$	$B_{\rm eff}$	$G_{\rm vib}$	$B_{\rm eff}$
$(0, 0^0, 0)$	0	0.000[a]	0.4744	0.000[b]	0.4734
$(0, 1^{1e}, 0)$	1	110.903	0.4778	132.589	0.4759
$(0, 1^{1f}, 0)$	1	110.911	0.4820	132.596	0.4793
$(0, 2^0, 0)$	0	222.151	0.4861	270.392	0.4821
$(0, 2^{2e,f}, 0)$	2	224.258	0.4858	269.909	0.4820
$(0, 3^{1e}, 0)$	1	332.951	0.4876	409.431	0.4827
$(0, 3^{1f}, 0)$	1	332.969	0.4965	409.445	0.4895
$(0, 3^{3e,f}, 0)$	3	338.887	0.4921	410.661	0.4862
$(0, 4^0, 0)$	0	441.633	0.4991	551.730	0.4906
$(0, 4^{2e,f}, 0)$	2	444.535	0.4920	551.839	0.4903
$(0, 4^{4e,f}, 0)$	4	454.322	0.4981	554.435	0.4903
$(1, 0^0, 0)$	0	1031.774	0.4755	1034.584	0.4713
$(1, 1^{1e}, 0)$	1	1148.715	0.4752	1170.828	0.4735
$(1, 1^{1f}, 0)$	1	1148.723	0.4792	1170.834	0.4768
$(1, 2^0, 0)$	0	1266.196	0.4893	1311.796	0.4797
$(1, 2^{2e,f}, 0)$	2	1266.979	0.4827	1311.478	0.4794
$(0, 0^0, 1)$	0	1412.100	0.4710	1413.618	0.4698
$(0, 1^{1e}, 1)$	1	1512.600	0.4748	1537.272	0.4725
$(0, 1^{1f}, 1)$	1	1512.609	0.4792	1537.279	0.4760

Experiment: Merritt, Bondybey and Heaven, JPC A113, 13300 (2009)

BeOBe

Singlet spectrum

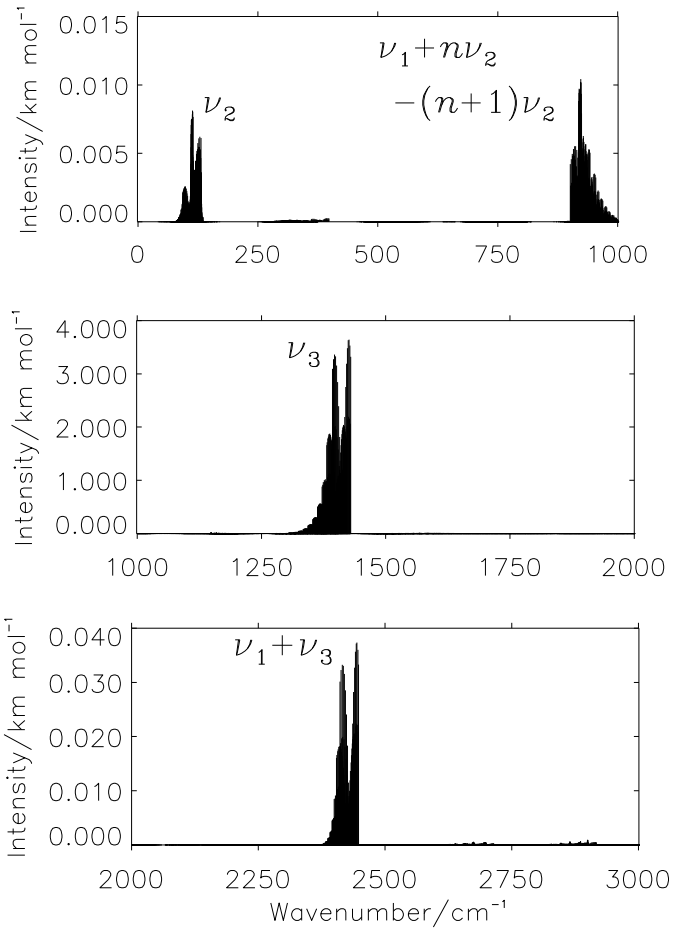

Triplet spectrum

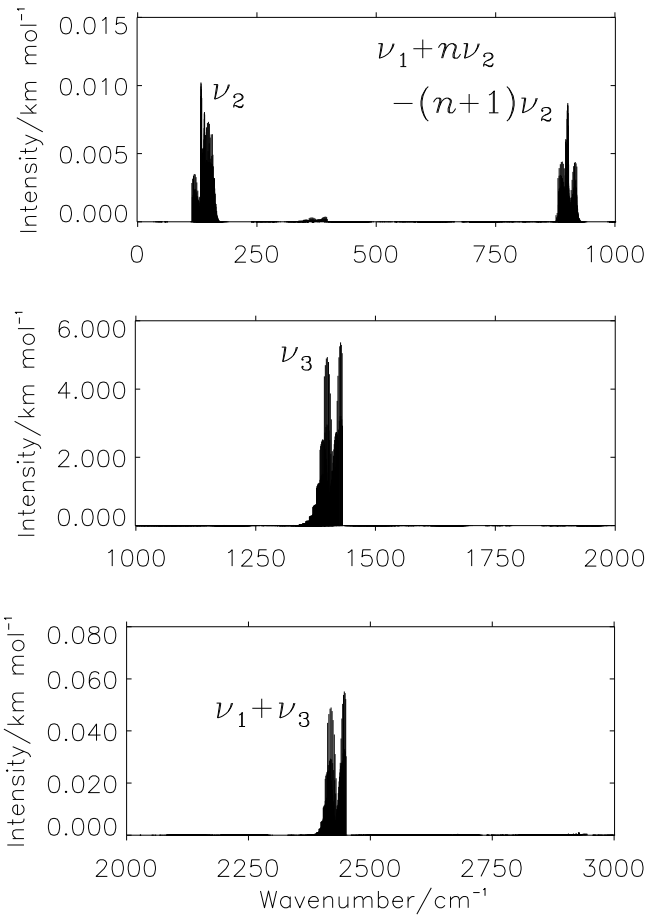

At 300 K. **All bands very weak**

MgOMg

$T_e(\tilde{a}) = 671\ cm^{-1}$

Diatomic
$^{24}Mg^{16}O$
774.7 cm^{-1}

The calculated vibrational term values $G_{vib} = E(v_1, v_2^{\ell_2}, v_3, N_{min} = \ell_2) - E(0, 0^0, 0, 0)$ and effective rotational constants B_{eff} (in cm^{-1}) for $^{24}Mg^{16}O^{24}Mg$ in the electronic states $\tilde{X}\,^1\Sigma_g^+$ and $\tilde{a}\,^3\Sigma_u^+$.

		$\tilde{X}\,^1\Sigma_g^+$		$\tilde{a}\,^3\Sigma_u^+$	
$(v_1, v_2^{\ell_2}, v_3)$	N_{min}	G_{vib}	B_{eff}	G_{vib}	B_{eff}
$(0, 0^0, 0)$	0	0.0[a]	0.1088	0.0[b]	0.1087
$(0, 1^{1e}, 0)$	1	77.1	0.1096	82.1	0.1094
$(0, 1^{1f}, 0)$	1	77.1	0.1099	82.1	0.1096
$(0, 2^0, 0)$	0	153.2	0.1107	165.5	0.1104
$(0, 2^{2e,f}, 0)$	2	155.2	0.1107	166.3	0.1103
$(0, 3^{1e}, 0)$	1	229.4	0.1113	249.4	0.1108
$(0, 3^{1f}, 0)$	1	229.4	0.1119	249.4	0.1114
$(0, 3^{3e,f}, 0)$	3	234.3	0.1116	252.2	0.1111
$(0, 4^0, 0)$	0	305.9	0.1126	335.4	0.1119
$(0, 4^{2e,f}, 0)$	2	307.4	0.1125	335.9	0.1118
$(0, 4^{4e,f}, 0)$	4	314.2	0.1126	339.9	0.1119
$(1, 0^0, 0)$	0	484.7	0.1086	484.5	0.1085
$(1, 1^{1e}, 0)$	1	568.0	0.1096	573.5	0.1090
$(1, 1^{1f}, 0)$	1	568.0	0.1090	573.5	0.1093
$(1, 2^0, 0)$	0	649.0	0.1103	659.7	0.1101
$(1, 2^{2e,f}, 0)$	2	651.9	0.1102	662.5	0.1099
$(0, 0^0, 1)$	0	915.0	0.1081	920.8	0.1080
$(0, 1^{1e}, 1)$	1	986.5	0.1089	997.1	0.1086
$(0, 1^{1f}, 1)$	1	986.5	0.1092	997.1	0.1089

MgOMg

Vertical excitation energies ΔE_{vert} (in cm^{-1}) of the low-lying singlet and triplet excited states of MgOMg, calculated at the FV-CAS(10,12)/MRCI+Q level of theory using the aug-cc-pCVQZ basis set. The calculations are carried out at the equilibrium geometry of the ground state ($\angle$(MgOMg) =180°; r_{e}(Mg-O) = 1.8014 Å). The singlet and triplet states are averaged in the state-average CAS procedure.

Singlet states State Φ^a		Configuration^b	ΔE_{vert}	$\Delta E_{\mathrm{vert}}{}^c$	$\lvert\langle\Phi\lvert\mu_x\rvert\tilde{X}\rangle\rvert^d$	$\lvert\langle\Phi\lvert\mu_y\rvert\tilde{X}\rangle\rvert^d$	$\lvert\langle\Phi\lvert\mu_z\rvert\tilde{X}\rangle\rvert^d$
$\tilde{X}\,{}^1\Sigma_g^+$	$1\,{}^1A_1$	$0.75\,\lvert 2\pi_u^4 6\sigma_g^2\rangle$	0	0	0.0	0.0	0.0
		$-\,0.55\,\lvert 2\pi_u^4 5\sigma_u^2\rangle$					
$A\,{}^1\Sigma_u^+$	$1\,{}^1B_2$	$0.88\,\lvert 2\pi_u^4 6\sigma_g^1 5\sigma_u^1\rangle$	23789	23788	0.0	1.47	0.0
		$-\,0.23\,\lvert 4\sigma_u^1 2\pi_u^4 6\sigma_g^1 5\sigma_u^2\rangle$					
$B\,{}^1\Sigma_g^+$	$2\,{}^1A_1$	$0.68\,\lvert 2\pi_u^4 5\sigma_u^2\rangle$	24269	24274	0.0	0.0	0.0
		$+\,0.51\,\lvert 2\pi_u^4 6\sigma_g^2\rangle$					
$\tilde{C}\,{}^1\Pi_g$	$1\,{}^1A_2$	$0.91\,\lvert 2\pi_u^3 6\sigma_g^2 5\sigma_u^1\rangle$	28783	28686	0.0	0.0	0.0
	$2\,{}^1B_2$	$+\,0.16\,\lvert 4\sigma_u^1 2\pi_u^3 6\sigma_g^2 5\sigma_u^2\rangle$			0.0	0.0	0.0
$\tilde{D}\,{}^1\Pi_g$	$2\,{}^2A_2$	$0.89\,\lvert 2\pi_u^4 6\sigma_g^1 2\pi_g^1\rangle$	28629	28705	0.0	0.0	0.0
	$3\,{}^1B_2$				0.0	0.0	0.0
$\tilde{E}\,{}^1\Pi_u$	$3\,{}^1A_1$	$0.81\,\lvert 2\pi_u^4 5\sigma_u^1 2\pi_g^1\rangle$	31912	31944	0.0	0.0	1.58
	$1\,{}^1B_1$	$-\,0.28\,\lvert 2\pi_u^3 6\sigma_g^1 5\sigma_u^2\rangle$			1.58	0.0	0.0
$\tilde{F}\,{}^1\Pi_u$	$4\,{}^1A_1$	$0.87\,\lvert 2\pi_u^3 6\sigma_g^1 5\sigma_u^2\rangle$	33524	33514	0.0	0.0	0.16
	$2\,{}^1B_1$	$+\,0.28\,\lvert 2\pi_u^4 5\sigma_u^1 2\pi_g^1\rangle$			0.16	0.0	0.0

Triplet states State Φ^a		Configuration^b	ΔE_{vert}	$\Delta E_{\mathrm{vert}}{}^c$	$\lvert\langle\Phi\lvert\mu_x\rvert\tilde{a}\rangle\rvert^d$	$\lvert\langle\Phi\lvert\mu_y\rvert\tilde{a}\rangle\rvert^d$	$\lvert\langle\Phi\lvert\mu_z\rvert\tilde{a}\rangle\rvert^d$
$\tilde{a}\,{}^3\Sigma_u^+$	$1\,{}^3B_2$	$0.93\,\lvert 2\pi_u^4 6\sigma_g^1 5\sigma_u^1\rangle$	775	791	0.0	0.0	0.0
$\tilde{b}\,{}^3\Pi_g$	$1\,{}^3A_2$	$0.82\,\lvert 2\pi_u^4 6\sigma_g^1 2\pi_g^1\rangle$	27414	27411	1.60	0.0	0.0
	$2\,{}^3B_2$	$-\,0.40\,\lvert 2\pi_u^3 6\sigma_g^2 5\sigma_u^1\rangle$			0.0	0.0	1.60
$\tilde{c}\,{}^3\Pi_g$	$2\,{}^3A_2$	$0.82\,\lvert 2\pi_u^3 6\sigma_g^2 5\sigma_u^1\rangle$	29479	29437	1.13	0.0	0.0
	$3\,{}^3B_2$	$+\,0.40\,\lvert 2\pi_u^4 6\sigma_g^1 2\pi_g^1\rangle$			0.0	0.0	1.13
$\tilde{d}\,{}^3\Pi_u$	$1\,{}^3A_1$	$0.87\,\lvert 2\pi_u^4 5\sigma_u^1 2\pi_g^1\rangle$	31687	31778	0.0	0.0	0.0
	$1\,{}^3B_1$	$+\,0.28\,\lvert 2\pi_u^3 6\sigma_g^1 5\sigma_u^2\rangle$			0.0	0.0	0.0
$\tilde{e}\,{}^3\Pi_u$	$2\,{}^3A_1$	$0.88\,\lvert 2\pi_u^3 6\sigma_g^1 5\sigma_u^2\rangle$	34272	34221	0.0	0.0	0.0
	$2\,{}^3B_1$	$-\,0.27\,\lvert 2\pi_u^4 5\sigma_u^1 2\pi_g^1\rangle$			0.0	0.0	0.0

420 nm 3.7 D

310 nm 4.0 D

360 nm 4.1 D

340 nm 2.9 D

Band Spectra of Magnesium Oxide and Hydroxide between 4000 and 3600 Å

MgOMg

By D. PESIC† and A. G. GAYDON
Chemical Engineering Department, Imperial College, London

MS. received 9th October 1958

Abstract. Band systems in the extreme violet have been excited in 'vacuum' arcs in oxygen, ordinary water vapour and heavy-water vapour, and also in a flame. Wavelengths of MgOH and MgOD bands are listed. An oxide system in the same region has been studied under large dispersion but is too complicated to analyse; it is attributed to a polyatomic emitter, possibly Mg_2O_2.

1959 Proc. Phys. Soc. 73 244

(http://iopscience.iop.org/0370-1328/73/2/313)

From Discussion:

must therefore conclude that a polyatomic emitter is responsible, at any rate for the main second group of bands. The species which can be expected are MgO_2, Mg_2O and Mg_2O_2. Although occurrence of these molecules in an arc at high temperature might appear unlikely (Brewer and Mastick 1951), similar molecules of the alkaline earth metals were found by a mass spectrometric method by Aldrich (1951) and Inghram and Chupka (1955).

MgOMg

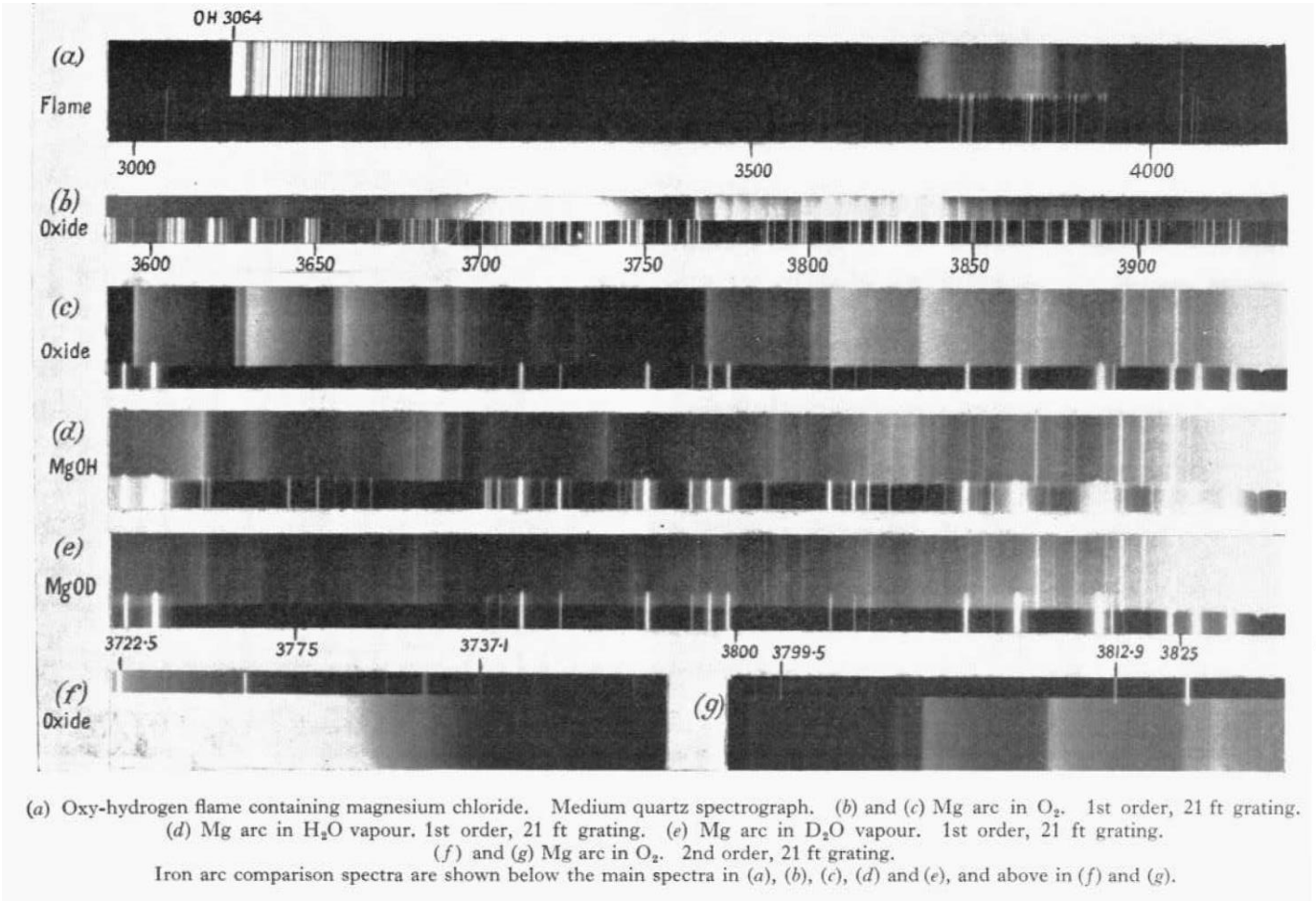

PROC. PHYS SOC. VOL. 72, PT. 2 (D. PESIC AND A. G. GAYDON)

(*a*) Oxy-hydrogen flame containing magnesium chloride. Medium quartz spectrograph. (*b*) and (*c*) Mg arc in O_2. 1st order, 21 ft grating. (*d*) Mg arc in H_2O vapour. 1st order, 21 ft grating. (*e*) Mg arc in D_2O vapour. 1st order, 21 ft grating. (*f*) and (*g*) Mg arc in O_2. 2nd order, 21 ft grating. Iron arc comparison spectra are shown below the main spectra in (*a*), (*b*), (*c*), (*d*) and (*e*), and above in (*f*) and (*g*).

$\tilde{A}^1\Sigma_u^+ - \tilde{X}$ 420 nm

$\tilde{E}^1\Pi_u - \tilde{X}$ 310 nm

$\tilde{b}^3\Pi_g - \tilde{a}$ 360 nm

$\tilde{c}^3\Pi_g - \tilde{a}$ 340 nm

CaOCa

JOURNAL OF MOLECULAR SPECTROSCOPY 68, 114–121 (1977)

Infrared Spectra of Matrix-Isolated Calcium-44 Substituted Oxides

LESTER ANDREWS[1] AND BRUCE S. AULT[2]

Chemistry Department, University of Virginia, Charlottesville, Virginia 22901

The products of ^{44}Ca atom reactions with ozone and oxygen have been isolated in solid nitrogen at 15 K. An excellent wavenumber fit for four isotopic molecules confirms the diatomic CaO assignment. Calcium and oxygen isotopic data strongly support the observation of rhombic $(CaO)_2$ and isosceles triangular CaO_2 and Ca_2O species.

Also think that spectrum shows linear CaCaO molecule

$^{40}Ca+^{16}O_3$

$^{44}Ca+^{16}O_3$

$^{44}Ca+55\%\ ^{18}O_3$

$^{44}Ca+55\%\ ^{18}O_2$

In solid N_2 *at 17* K

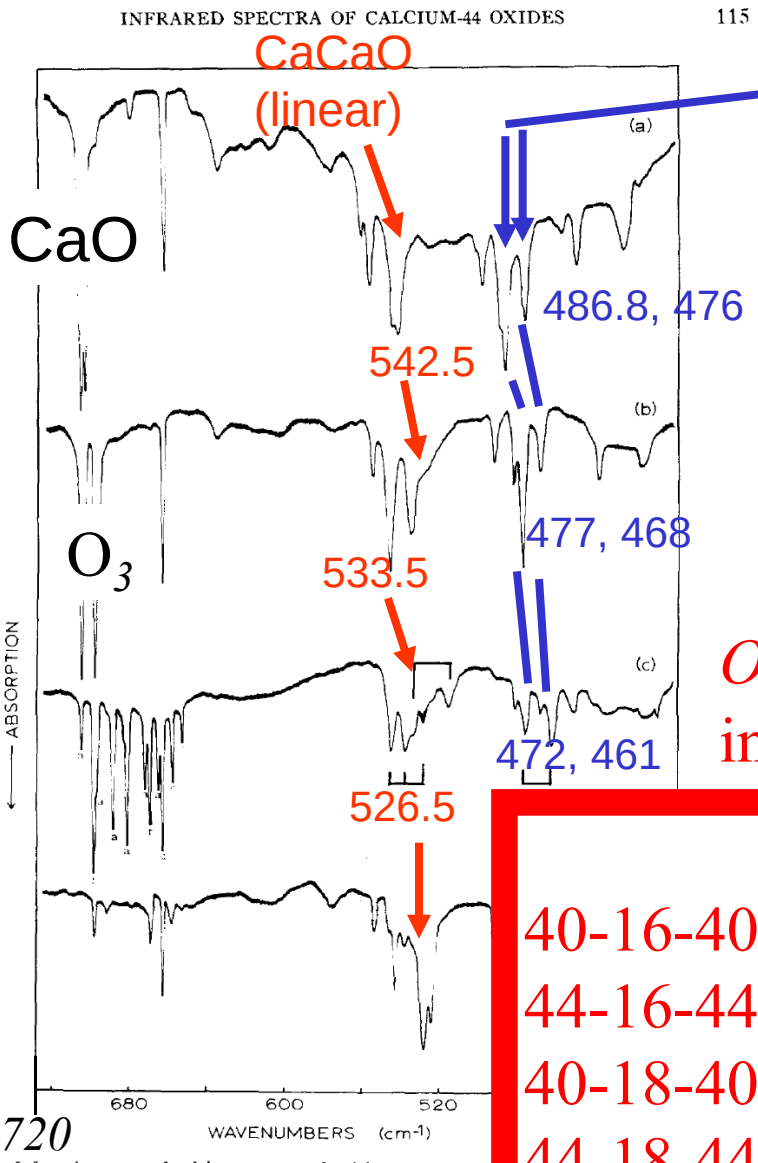

FIG. 1. Infrared spectra of calcium–ozone and calcium–oxygen rea
at 15 K. Spectrum (a) natural ^{40}Ca and $N_2/^{16}O_3$ = 130/1. Trace (b) ^{44}Ca
(c) ^{44}Ca and $N_2/^{16,18}O_3$ = 150/1, 55% ^{18}O enrichment. Trace (d) ^{44}Ca a

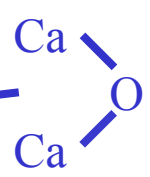

120^0 bent

$^{40}Ca^{16}O$
$\upsilon = 722.4\ cm^{-1}$
in gas phase
$\upsilon = 707\ cm^{-1}$
in N_2 *matrix.*

Our results for CaOCa *in the* $\tilde{X}^1\Sigma_g^+$ *state:*

	υ_1	υ_2	υ_3
40-16-40	345	55	755
44-16-44	330	55	749
40-18-40	344	52	719
44-18-44	329	52	713

SrOSr singlet-triplet interaction

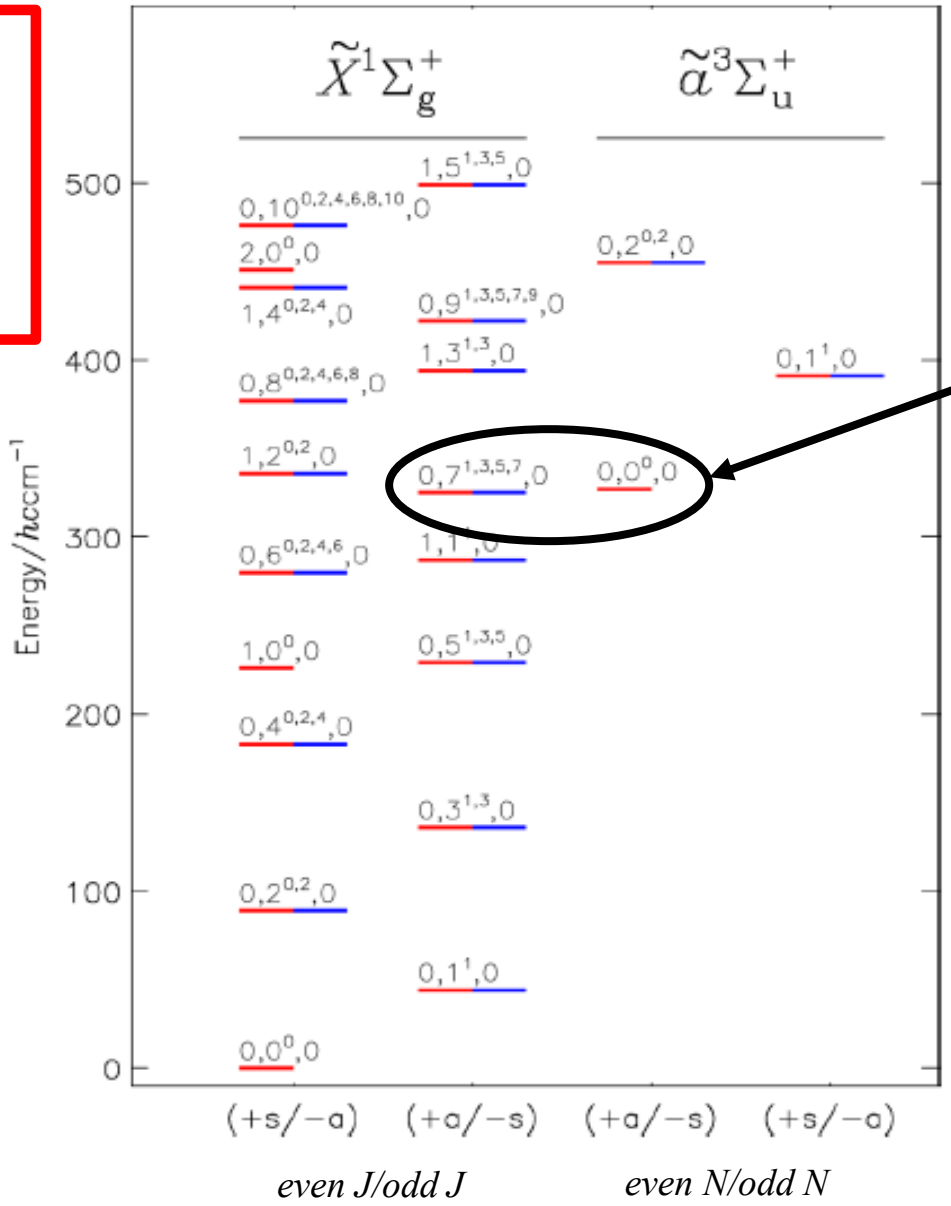

S-T interaction?

$\Delta E \sim 2$ cm^{-1}

What is S-T matrix element?

SrOSr

ST matrix element = = –0.01 cm^{-1}

$$\langle (\nu_2^{(\tilde{a})})^{l_2^{(\tilde{a})}} | \hat{H}_{SO} | (\nu_2^{(\tilde{X})})^{l_2^{(\tilde{X})}} \rangle = \int_0^{\pi} \psi_{bend}^{(\tilde{a})}(\rho) \langle \Psi_{elec}^{(\tilde{a})} | \hat{H}_{SO} | \Psi_{elec}^{(\tilde{X})} \rangle_{el} \psi_{bend}^{(\tilde{X})}(\rho)\, d\rho$$

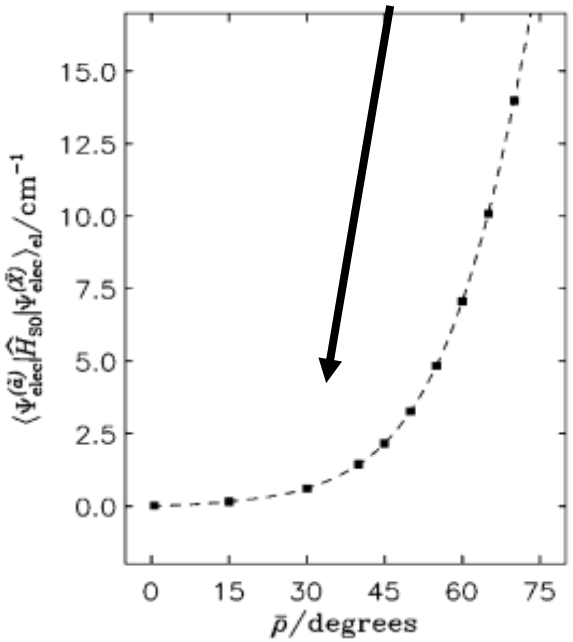

Figure 5. Values of $\langle \Psi_{elec}^{(\tilde{a})} | \hat{H}_{SO} | \Psi_{elec}^{(\tilde{X})} \rangle_{el}$ computed with MOLPRO for $r_1 = r_3 = 2.15$ Å are represented as filled squares. A cubic spline function determined to reproduce the ab initio values is plotted as a dashed curve.

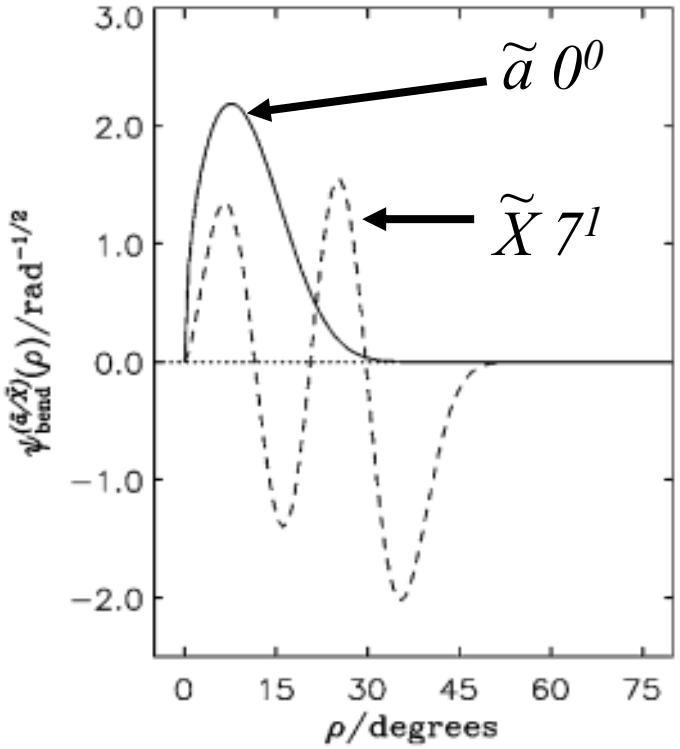

ΔE ~ 2 cm^{-1} Thus energy shift ~ $(0.01)^2/2$ cm^{-1} = 0.00005 cm^{-1}

MOM equilibrium bond length

S-T splitting

	$r_e^{\tilde{X}}$ / Å		E_{CBS}	$\langle \Psi_{\mathrm{elec}}^{(\tilde{a})} \mid \hat{H}_{\mathrm{SO}} \mid \Psi_{\mathrm{elec}}^{(\tilde{X})} \rangle_{\mathrm{el}}$	
				180°	140°
BeOBe	1.409		280	0.002	0.2
MgOMg	1.801		656	0.007	0.7
CaOCa	1.995		307	0.002	0.4
SrOSr	2.150		344	0.006	1.9
BaOBa	2.201		510	0.064	11.7
RaORa	2.280		601	0.265	51.6

BaOBa bending potential energy curves

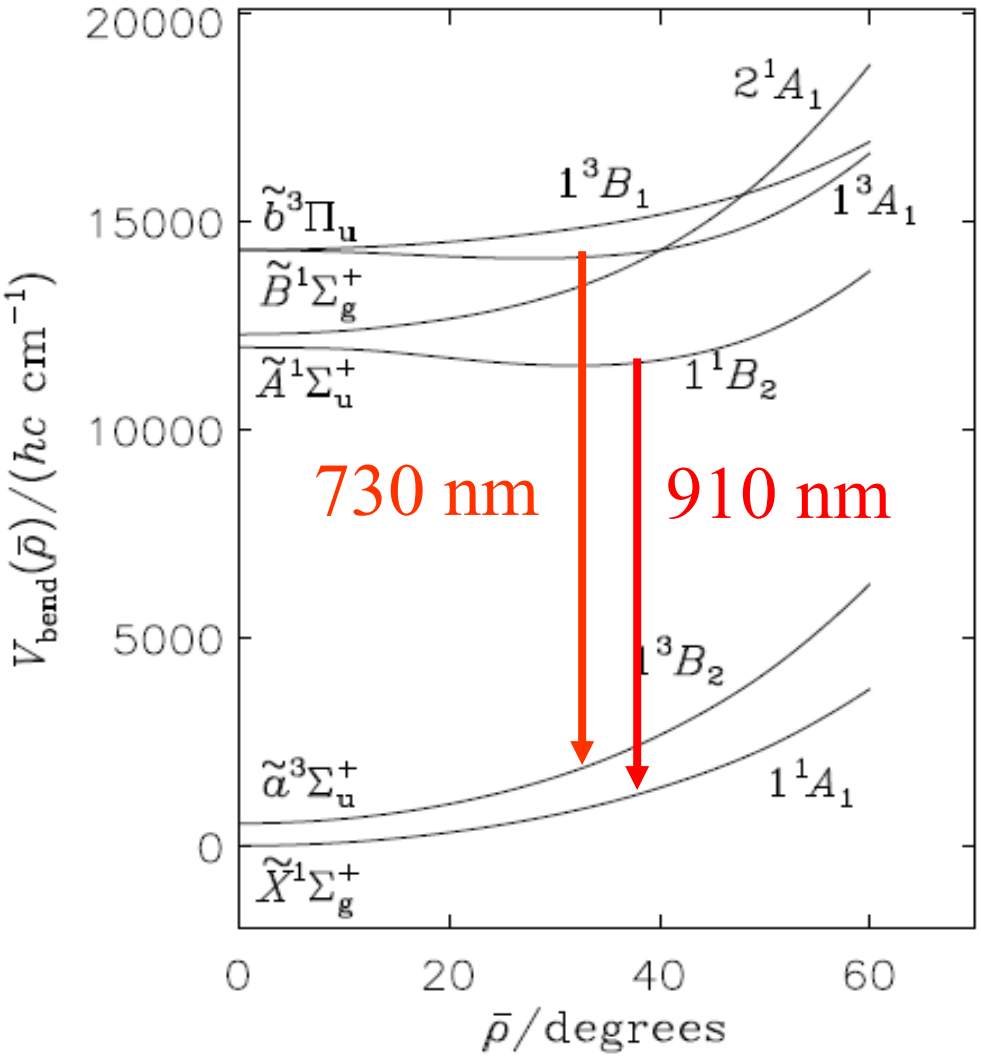

$Ba^{0.5+}\ O^{-}\ Ba^{0.5+}$

Predicted emission wavelengths

Gee et al. *J. Phys. Chem., Vol. 100, No. 32, 1996*

BaOBa

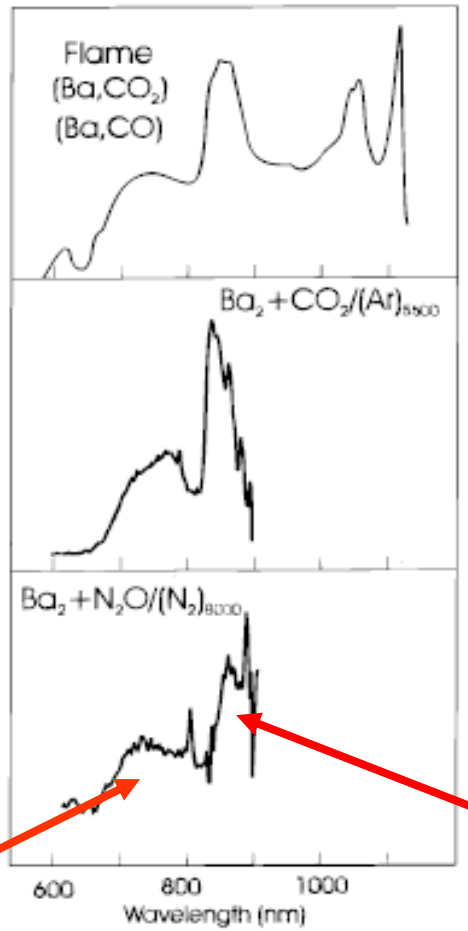

Triplet Emission ~700 nm

Singlet Emission ~900 nm

Figure 8. Comparison of the fluorescence spectra assigned in the present work to Ba_2O with that observed by West et al.[6] (upper part) in Ba/CO_2 and Ba/CO flames. The spectra have been corrected for the transmission of the detection system. The middle part corresponds to the reaction $Ba_2 + CO_2$ on argon clusters and the bottom part to the $Ba_2 + N_2O$ reaction on nitrogen clusters.

The cluster isolated chemical reaction technique.

West and Poland JCP 66, 2139 (1977)

Spring has arrived in Wuppertal!

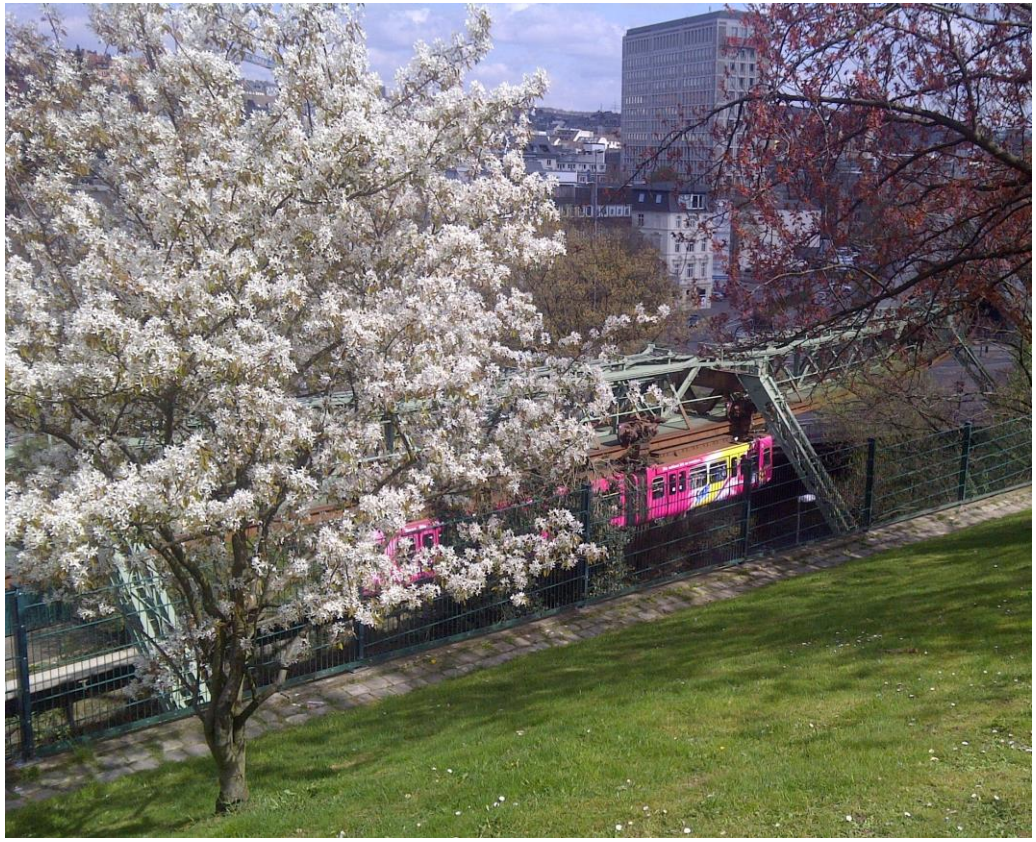

Thank you for your attention!